

UC San Diego

UC San Diego Previously Published Works

Title

Transportome remodeling of a symbiotic microalga inside a planktonic host.

Permalink

<https://escholarship.org/uc/item/414627z9>

Journal

The ISME Journal, 18(1)

Authors

Juéry, Caroline

Auladell, Adria

Füßy, Zoltan

et al.

Publication Date

2024-01-08

DOI

10.1093/ismejo/wrae239

Peer reviewed

Transportome remodeling of a symbiotic microalga inside a planktonic host

Caroline Juéry^{1,*}, Adria Auladell², Zoltan Füssy^{3,4}, Fabien Chevalier¹, Daniel P. Yee¹, Eric Pelletier^{5,6}, Erwan Corre⁷, Andrew E. Allen^{3,4}, Daniel J. Richter², Johan Decelle^{1,*}

¹Cell and Plant Physiology Laboratory, Unité Mixte de Recherche (UMR) 5168 Centre de l'Energie Atomique (CEA)-Centre national de la recherche scientifique (CNRS)-University Grenoble Alpes—INRAE, 38000, Grenoble, France

²Institut de Biologia Evolutiva (Consejo Superior de Investigaciones Científicas-Universitat Pompeu Fabra), 08003 Barcelona, Spain

³Scripps Institution of Oceanography, University of California San Diego, La Jolla, 92037 CA, United States

⁴Microbial and Environmental Genomics, J. Craig Venter Institute, La Jolla, 92037 CA, United States

⁵Génomique Métabolique, Genoscope, Institut de Biologie François-Jacob, CEA, CNRS, University Evry, Université Paris-Saclay, 91000 Evry, France

⁶Research Federation for the study of Global Ocean Systems Ecology and Evolution, FR2022/Tara GOsee, 75000 Paris, France.

⁷Centre National de la Recherche Scientifique/Sorbonne Université, Station Biologique de Roscoff, 29680 Roscoff, France

*Corresponding authors: Caroline Juéry, Cell and Plant Physiology Laboratory, Centre National de la Recherche Scientifique, 17 avenue des Martyrs, 38000 Grenoble Email: carolinejuery@gmail.com and Johan Decelle, Cell and Plant Physiology Laboratory, Centre National de la Recherche Scientifique—17 avenue des Martyrs, 38000, Grenoble, France. Email: johan.decelle@univ-grenoble-alpes.fr

Abstract

Metabolic exchange is one of the foundations of symbiotic associations between organisms and is a driving force in evolution. In the ocean, photosymbiosis between heterotrophic hosts and microalgae is powered by photosynthesis and relies on the transfer of organic carbon to the host (e.g. sugars). Yet, the identity of transferred carbohydrates as well as the molecular mechanisms that drive this exchange remain largely unknown, especially in unicellular photosymbioses that are widespread in the open ocean. Combining genomics, single-holobiont transcriptomics, and environmental metatranscriptomics, we revealed the transportome of the marine microalga *Phaeocystis* in symbiosis within acantharia, with a focus on sugar transporters. At the genomic level, the sugar transportome of *Phaeocystis* is comparable to non-symbiotic haptophytes. By contrast, we found significant remodeling of the expression of the transportome in symbiotic microalgae compared to the free-living stage. More particularly, 36% of sugar transporter genes were differentially expressed. Several of them, such as GLUTs, TPTs, and aquaporins, with glucose, triose-phosphate sugars, and glycerol as potential substrates, were upregulated at the holobiont and community level. We also showed that algal sugar transporter genes exhibit distinct temporal expression patterns during the day. This reprogrammed transportome indicates that symbiosis has a major impact on sugar fluxes within and outside the algal cell, and highlights the complexity and the dynamics of metabolic exchanges between partners. This study improves our understanding of the molecular players of the metabolic connectivity underlying the ecological success of planktonic photosymbiosis and paves the way for more studies on transporters across photosymbiotic models.

Keywords: planktonic photosymbiosis, transporters, carbon exchange, single-cell transcriptomic, microalga, sugars, protists, metatranscriptomics

Introduction

Symbiosis between a heterotrophic host and a photosynthetic partner (photosymbiosis) is considered to be the primary event which led to the acquisition and distribution of plastids in the evolution of eukaryotes [1, 2]. Photosymbiosis remains an essential life strategy and supports the functioning of today's aquatic ecosystems especially in oligotrophic waters [3–6]. This partnership, considered as either mutualism or farming in the spectrum of symbioses [5, 7], can provide a competitive advantage in a nutritionally challenging environment where nutrients and preys are scarce (oligotrophic waters). Therefore, partners need to establish a metabolic connection in order to exchange metabolites and nutrients. The microalgae need to be supplied by the host with all the essential macro- and micro-nutrients (e.g. iron, nitrogen) to maintain their metabolic and physiological activity. In turn, the

host can benefit from photosynthetic products (photosynthates) exported from the microalgae [8].

In the past decade, NanoSIMS (Nanoscale Secondary Ion Mass Spectrometry) studies coupled with ¹³C labeling improved our knowledge on carbon transfer and allocation in different photosymbiotic systems [9–11]. Transferred photosynthates have been mostly investigated in benthic multicellular photosymbioses such as reef-dwelling invertebrates (e.g. anemones, jellyfish, giant clams, corals) living with Symbiodiniaceae microalgae. Sugars, which are the main photosynthetic products, and lipids are considered to be the main photosynthates exported from the symbiotic microalgae [12–14]. Glucose has been shown to be a major transferred metabolite in some photosymbioses [15, 16], as well as inositol or galactose [17, 18]. Glycerol has also been suggested as a putative transferred metabolite since it is

Received: 31 May 2024. Revised: 7 October 2024. Accepted: 9 December 2024

© The Author(s) 2024. Published by Oxford University Press on behalf of the International Society for Microbial Ecology.

This is an Open Access article distributed under the terms of the Creative Commons Attribution License (<https://creativecommons.org/licenses/by/4.0/>), which permits unrestricted reuse, distribution, and reproduction in any medium, provided the original work is properly cited.

significantly released by free-living Symbiodiniaceae in culture [19–21]. However, the exact nature of translocated carbohydrates is still uncertain since experimental evidence is difficult to obtain on such photosymbiotic systems and on these very rapid metabolic processes.

In symbiosis, both partners need to reprogram their transportome (defined as “membrane proteins responsible of the translocation of any kind of solutes across the lipid layer” [22]) in order to establish metabolic connectivity. Most metabolites including sugars require a complete set of transporters to traverse algal and host membranes. For example, in symbioses between plants and fungi, changes in expression of the transporter genes are essential to connect and integrate different metabolisms [23]. In marine photosymbioses, some transporters have been highlighted in genomic [24] and transcriptomic studies [25]. A glucose transporter (*GLUT8*) and an aquaporin (*GfIP*) that could putatively transport glycerol, were described in anemones and the jellyfish *Cassiopea* [26, 27]. Even though most studies have focused on host transporters, less is known about the ones of the symbiotic microalgae that can export energy-bearing metabolites derived from photosynthesis. So far, a Sugars Will Eventually be Exported Transporter (*SWEET*) has been described as a glucose transporter located in the cell membrane of the microalga *Breviolum* (Symbiodiniaceae), the symbiont of the anemone *Exaiptasia diaphana* [28].

Relatively less studied than reef ecosystems, a wide diversity of photosymbioses are also found in marine and freshwater plankton. For instance, radiolarians and foraminiferans that are widespread in the sunlit layer of the ocean can host diverse microalgae [29]. Among radiolarians, some species of acantharia live in symbiosis with different species of *Phaeocystis* (Haptophyta) depending on the oceanic regions [30]. For instance, *P. cordata*, *P. globosa*, and *P. antarctica* are known to be abundant in their free-living phase, and are found in symbiosis when acantharia are present (e.g. *P. antarctica* is the symbiont in the Southern Ocean [31]). Symbiotic acantharia significantly contribute to primary production (up to 20% in surface oligotrophic oceans) and carbon fluxes to deep layers of the ocean [32, 33]. Previous studies using 3D electron microscopy have shown that the microalga *Phaeocystis* undergoes drastic morphophysiological changes in symbiosis: cell and plastid volume, as well as plastid number, greatly increased compared to free-living cells in culture [34]. Whereas cell division is very likely arrested in symbiosis, photosynthesis and carbon fixation are enhanced, corroborated by an upregulation of many genes of the Calvin–Benson cycle [34]. Symbiotic microalgae with their expanded photosynthetic apparatus therefore produce a substantial amount of organic carbon but the identity of these compounds and the mechanisms by which they are transferred to the host remain largely unknown. Investigating the composition and expression of the algal transportome can reveal how symbiotic microalgae metabolically connect to their host and can provide insights on the putative exchanged metabolites.

Here, we conducted genomic and transcriptomic analyses on an uncultivable planktonic photosymbiosis between the microalga *Phaeocystis* and acantharia hosts in order to shed light on the molecular mechanisms of their metabolic connectivity. More specifically, we investigated whether the algal transportome is remodeled in symbiosis. We first compared sugar transporter genes in haptophyte genomes and studied their expression in free-living and symbiotic stages of *Phaeocystis* using a combination of single-holobiont transcriptomics and in situ environmental metatranscriptomics. We evaluated the transcriptional dynamics of these sugar transporters in symbiosis at different periods of the

day. This study reveals that the transportome of the microalga is significantly remodeled in symbiosis within a host and pinpoints putative key sugar transporters with different transcriptional patterns during the day. This work significantly improves our understanding of the metabolic connectivity between a host and microalgae, and so provides fundamental knowledge of the ecological success of this widespread symbiosis in the ocean.

Material and methods

Dataset of genomic sequences of haptophyte transporters

Genomic identification of transporter genes was obtained from a re-annotation of the 186 115 protein sequences of six haptophyte species (*Diacronema lutheri*, *Emiliania huxleyi*, *Chrysochromulina tobinii*, *Phaeocystis antarctica*, *Phaeocystis globosa* from Phycocosm [35] and *Phaeocystis cordata* from [36]). Sequences were re-annotated with multiple tools in order to have a complete description of each transporter useful for downstream analysis: InterProScan 5.60 with best scores for *P*-values < .000001 [37], Transporter Classification Database [38], blastp of the protein sequences with diamond (2.1.7, options: -e 0.00001—ultra-sensitive—max-target-seqs 1), to the Uniprot release 2022 02, Hmmscan with Pfam-A.hmm 2021-11-15 [39], EggNog mapper [40]. To identify transporters, we first searched in the merged files of annotations for the terms: “carrier|transport|channel|permease|symporter|exchanger|antiporter|periplasmic|facilitator”. We searched sugar transporters using terms such as: “disaccharide|carbohydrate|sugar|ose|saccharide|glucose|polysaccharide”.

We used Phobius [41] and tmhmm 2.0 [42] to predict the number of transmembrane domains. We selected proteins that presented at least two transmembrane domains and less than three differences in terms of transmembrane domain number between Phobius and tmhmm. For PF00083 and PF07690 families, we used protein models (from InterPro database, <https://www.ebi.ac.uk/interpro/>) of the subfamilies domains described in Table S1, in order to build hmm profiles and use hmmsearch (best value, *P*-value E-23) to carefully identify these transporters. Subcellular localization of *P. cordata* transporters was evaluated through five different tools: Deeploc 2.0 [43], TargetP 2.0 [44], Hectar 1.3 [45], WoLF PSORT [46], and MuLocDeep 1 [47]. We used two thresholds: (i) a Deeploc score > 0.5 (as used in [48]) and (ii) the consistency of prediction should be the same for at least two tools, to select the most accurate putative predictions of transporter localization.

Single-holobiont transcriptomics: sampling and analysis

For the free-living stage, a total of nine replicates of *P. cordata* cells (strain RCC1383 from the Roscoff Culture Collection) maintained in K2 medium at 50–60 $\mu\text{mol photons m}^{-2} \text{s}^{-1}$ and 20°C were harvested at 7 p.m. at both late and stationary growth stages. Symbiotic acantharians (holobionts) with intra-cellular *P. cordata* were collected with a 150 μm plankton net in the Mediterranean Sea at Villefranche-sur-Mer, France. Individual holobionts were manually isolated with a micropipette under a binocular microscope, rapidly transferred into filtered seawater (0.2 μm), and maintained in an incubator (50–75 $\mu\text{mol photons m}^{-2} \text{s}^{-1}$, 20°C, 12 h/12 h). Free-living and symbiotic samples were frozen in the same conditions, in liquid nitrogen in a 0.2 μl polymerase chain reaction (PCR) tube containing 4.4 μl of Smart-Seq2 buffer (Triton X-100 0.4% / RNase inhibitor (ratio 19/1), dNTPs 10 mM, oligo dT 5 uM, [49]). Each sample was sequenced at 75 million reads, 2 × 150

paired-end with an Illumina NextSeq 500 instrument. A total of 1.9 billion reads were produced for this study.

In order to identify the symbiotic microalgae, we retrieved 18S ribosomal ribonucleic acid (rRNA) sequences in the assemblies of each samples using Barmap (v0.9, Seemann T., Booth T. <https://github.com/tseemann/barmap>) and taxonomically identified them using vsearch on the Pr2 database v2 [50] (Table S7).

Reads were first trimmed using trimmomatic (version 0.39, option PE -phred33; ILLUMINACLIP: contams_forward_rev.fa:2:30:10 LEADING:3 TRAILING:3 SLIDINGWINDOW:4:15 MINLEN:36 [51]) and bacterial, virus, human, and fungal sequence contaminants removed using kraken2 (2.1.2) and the k2_standard_202310 database [52]. In order to maximize the mapping rates of the reads, we built a new reference transcriptome of *P. cordata* from the reads obtained with the sequencing of our culture (strain RCC1383 from the Roscoff Culture Collection) plus the reads from the PRJNA603434 BioProject deposited at NCBI GenBank [34] from the same *Phaeocystis* strain. Briefly, reads were assembled using maSPAdes v3.15.5 [53] and peptides were predicted using TransDecoder v5.7.1 and Transdecoder.Predict [54] using the Pfam. A database and UniProt (3A-2022) database to identify accurate protein coding sequences. The peptides were annotated with the same method as for the genomic proteome. Conserved orthologous scores were calculated with BUSCO v5.4.4 [55] and re-alignment rates with Bowtie2 [56]. We reached a 68.87% re-mapping rate of the reads (31.13% with the previous reference, Fig. S2); the two transcriptome references (this study and [34]) presented the same completeness (BUSCO score, Fig. S2 and [34]).

To verify if the decontamination of the reference transcriptome step using kraken2 was sufficient, we applied two blastp searches of the predicted peptides (as queries): (i) against the *P. cordata* protein sequences from the Joint Genome Institute's genome portal; and (ii) against the NCBI nr database. For the 330 transcripts annotated as sugar transporter in the reference transcriptome, 96% of them were found in the protein sequences of *P. cordata* genome. The contigs presenting <50% identity (4 contigs) have a NCBI blast with *Oryza sativa*, *Arabidopsis thaliana*, and 2 bacteria but with a percentage of identity very close to the one found with the blastp against the *P. cordata* genome-derived protein models. For the 14 proteins not found in the *P. cordata* genome, only 4 have an NCBI match with a bacterial assignment but again with a < 50% identity. Thus, in total, six sugar transporter genes putatively presented a bacterial homolog but with ~35% identity on average (Table S1, "Blastp refTrans JGIgenome").

For the Differential Expression (DE) analysis, read counts were obtained using Kallisto (0.48.0, [57]) on the reference transcriptome coding sequences. Prior to the DE analysis, a supplementary step of normalization was conducted using preprocesCore R package that enables a quantile normalization (see MA plot Fig. S3 for counts distribution). The differential gene expression analysis between free-living vs symbiotic stages was conducted using the DESeq2 R package (1.36.0, [58]). We used the threshold of normalized read counts >10 among all replicates to qualify a gene as expressed in a given condition [34].

Tara oceans metatranscriptomic data analysis

Reads of the Mediterranean stations 11, 9, 22, 23, 25, and 30 of the Tara Oceans expedition (2009–2014) were obtained from the published dataset (PRJEB402/ERP006152, [59]). To compare the expression of sugar transporter genes between two size fractions, we transformed their TPM values into ratios between the expression of genes of interest and housekeeping genes that we identified in a similar way to the approach used by quantitative PCR (Table S4

"HousekeepingGenes"). Briefly, the community expression patterns are compositional data, not absolute counts, and this type of data is constrained to an arbitrary fixed total defined by the sequencing depth, creating potentially spurious correlations through changes in abundance of other organisms in the system (see [60] for a review on the topic). A solution to this problem is to analyze ratios of gene expression instead of the proportions of the total. In this approach, choosing an appropriate denominator (housekeeping genes) to calculate ratios is critical [61]. We established a robust denominator via 4 criteria: (i) analyzing only samples in which at least 20% of the *Phaeocystis* transcriptome was expressed and retained only genes expressed in all samples showing at least 20% *Phaeocystis* expression in every analyzed sample (this procedure eliminated 7 of the top 19 genes with the most reads mapped, likely because their high expression was the result of non-specific mapping in samples in which <20% of the *Phaeocystis* transcriptome was expressed), (ii) selecting genes whose expression across all analyzed samples has a coefficient of variation below 200 (mean CV all genes = 374.8) and a fold change from the mean below 2, (iii) checking that the genes present a functional annotation corresponding to typical housekeeping genes, and (iv) checking that the genes correlate enough between them and through a k-means clustering, selecting the cluster with the highest amount of genes presenting $r > 0.5$ (adapting [61]). We then used the sugar transporters' TPM as a numerator and the geometric mean of the housekeeping selected genes as a denominator to calculate our statistics. See also supplemental file Figs S6 and S7 and Table S6 where additional information on the method for this analysis.

Temporal transcriptional dynamics of sugar transporters of the microalga *Phaeocystis cordata*

To evaluate the expression of the sugar transportome during the day, we collected more symbiotic acantharia in surface waters of the Mediterranean Sea (Villefranche-sur-Mer, France). For "Morning" samples, we sampled and isolated acantharia, maintained them in an incubator overnight (50–75 $\mu\text{mol PAR m}^{-2} \text{s}^{-1}$, 20°C, 12 h/12 h), and harvested them the day after at 9 a.m. in the morning (one hour of light exposure). For "evening" samples, symbiotic acantharia were collected, and isolated in filtered seawater, and frozen the same day ~7 p.m. in the evening after 10 hours of light in the incubator. For "dark-evening" samples, holobionts were collected and maintained in the incubator with light until 8 p.m., and then transferred into a black box until 7 p.m. the following day. In order to compare gene expression across time/light conditions (morning, evening, and dark-evening), we built a matrix of read counts for the three conditions using kallisto on the reference transcriptome of *P. cordata*, as explained above, and normalized these counts using DESeq2 R package without "reference condition" for the dds object creation.

Results and discussion

Genomic inventory of sugar transporters in *Phaeocystis* species

To identify the molecular toolbox underlying metabolic fluxes and investigate the putative genomic footprint of symbiosis, we unveiled the transportome of *Phaeocystis* (three species: *P. antarctica*, *P. cordata*, *P. globosa*) at the genomic level, and we compared this transportome with three non-symbiotic haptophyte species (*E. huxleyi*, *C. tobinii*, and *D. lutheri*; Fig. 1A). We also predicted subcellular localization of transporters using a combination of

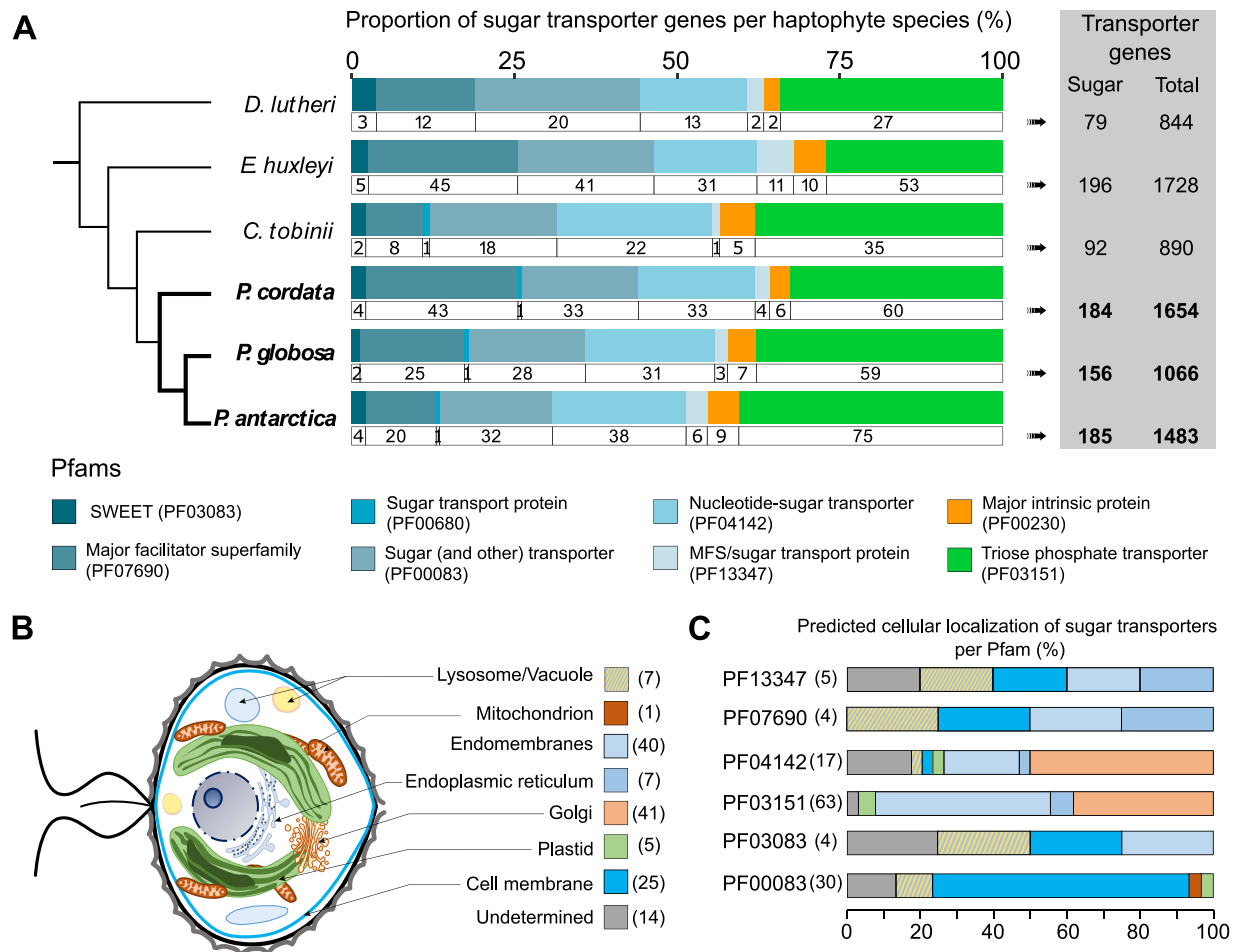


Figure 1. Genomic composition of sugar transporters of six haptophyte species. (A) Gene composition and Pfam families of different sugar transporters identified in the genomes of six haptophytes species represented in a schematic phylogenetic tree (*D. lutheri*, *E. huxleyi*, *C. tobinii*, *P. antarctica*, *P. globosa*, *P. cordata*). Eight Pfam families were found and represented by different colors and the number of sugar transporter genes within each Pfam is indicated. The genus *Phaeocystis* comprise between 156 and 184 sugar transporters out of 1066 to 1654 transporters in total. (B) In *P. cordata*, the subcellular localization and number of sugars transporters are shown in the schematic drawing of the microalga (prediction using a combination of *in silico* tools, see Materials and methods and Table S1). (C) Proportion of sugar transporters within each compartment of the cell for each Pfam family.

different *in silico* tools. We particularly focused on sugar transporters, since soluble sugars may be the main exported currency to the host. Using the same method of protein annotation for each species, we identified transporters based on the presence of transmembrane domains and protein domain annotations using the InterPro/Pfam classification. In total, we found 270 unique Pfam domains for the transporter genes in haptophyte genomes. The three different *Phaeocystis* species analyzed here contained an average of 965 transporter genes corresponding to 3% of all genes (1244 genes or 4% if we include those lacking a predicted transmembrane domain, see Methods, Fig. 1A, Table S1: “General values1” and “General values2 (TMD)”).

Across *Phaeocystis* genomes, sugar transporter genes represented on average 18% (175 out of 965) of all transporter genes and were classified into eight different core Pfams (i.e. shared among all haptophyte species, Fig. 1A, Table S1: “General values2 (TMD)”). The largest Pfam family of sugar transporters is the Triose Phosphate Transporters (TPT, PF03151) with 64.7 genes on average across *Phaeocystis* species, similar to *E. huxleyi*, but higher than in diatom genomes (between 13 and 22 TPTs for *Phaeodactylum tricorutum* [62, 63]). In plants, TPTs are transporters located in the plastid envelope and export photosynthetically-derived sugars to the cytosol [64]. For *P. cordata*, *in silico* subcellular localization analyses predicted only three out of 60 TPTs associated to the

plastid membranes whereas the majority were predicted to be located in the endomembrane system (Golgi apparatus or endoplasmic reticulum, ER; Fig. 1C Table S1). Similar to diatoms, the localization of TPTs in the four membranes of the secondary red plastid of *Phaeocystis* remains ambiguous and TPTs could also be localized elsewhere in the cell [65–67].

The second largest sugar transporter family was the “Sugar (and Other) transporters” Pfam: PF00083, containing 31 genes in *Phaeocystis* on average (41 in *E. huxleyi*, Fig. 1A). This Pfam is composed of different transporters with various substrates, such as glucose, galactose, mannose, polyol, and inositol sugars [68, 69]. For instance, using a complementary hidden Markov model (HMM) search of InterPro domains in *P. cordata* PF00083 proteins, we found 5 GLUT transporter (IPR002439), 6 sugar transporter ERD6/Tret1-like (IPR044775), and 12 Sugar transport protein STP/Polyol transporter PLT (IPR045262) domains (Table S1: “GLUTcharacterization”). *In silico* subcellular localization successfully assigned a prediction for 21 of the 33 transporter genes from PF00083 of *P. cordata* in the cell membrane, three in vacuoles, and one in the plastid membrane (Fig. 1B). These results suggest that some of these transporters might be involved in sugar flux at the cell surface. Nucleotide-sugar transporters (NSTs, PF04142) play an important role in the biosynthesis of glycoproteins, glycolipids, and non-cellulosic polysaccharides

translocating nucleotide-sugars to the Golgi apparatus [70, 71]. In *Phaeocystis* species, we found 34 NSTs genes on average (31 in *E. huxleyi*). In *P. cordata*, 50% of the NSTs were predicted to be localized to the Golgi apparatus, in accordance with their known biological function (Fig. 1C).

SWEET transporters (PF03083) are bidirectional transporters of small sugars following the concentration gradient [72]. SWEETs have been highlighted in terrestrial and aquatic symbioses (Fabaceae-*Rhizobium*, cnidarians-Symbiodiniaceae), particularly in sugar efflux from the photosynthetic to the heterotrophic partner [28, 73–75]. Between two and four SWEET genes were found across *Phaeocystis* genomes. Among the four SWEET of *P. cordata*, one was predicted in the lysosome/vacuole, one in the endomembrane system, and one in the cell membrane. For the Pfam PF13347 (MFS/sugar transport protein) [76, 77], we found four genes in *Phaeocystis* genomes.

We investigated the presence of putative sugar transporters from the Major Facilitator Superfamily PF07690 (MFS). Through an HMM search (Table S1, “PF07690_characterization”), we detected 43 putative sugar transporters for *P. cordata* and 25 and 20 for *P. globosa* and *P. antarctica*, respectively. Among them, many genes corresponded to glucose-6-phosphate transporter (SLC37A1/SLC37A2, IPR044740). In *Phaeocystis*, most of these PF07690 transporters were predicted to be either at the cell membrane or ER (Table S1, “Subcellular Localization P.cord”). Finally, we investigated the presence of genes belonging to PF00230 that correspond to a specific type of aquaporin, found to be involved in different reef photosymbioses for putative glycerol transport (anemones, jellyfish, and giant clams [26, 27, 78]). In *Phaeocystis* genomes, seven (*P. cordata*) to nine (*P. antarctica*) homologs of these aquaporin genes were found.

This inventory of sugar transporters in haptophyte genomes unveiled different categories that could be involved in the influx and efflux of sugars in the microalga *Phaeocystis*. Overall, 25 sugar transporters were predicted to be localized at the cell membrane (Fig. 1B), and the vast majority presented a putative localization in the endomembrane system (including ER or Golgi). We also hypothesize that sugar transporters can be located on vesicles from the endomembrane system that could fuse to the cell membrane [79]. These predictions provide some localization patterns for the different categories of sugar transporters in *Phaeocystis* but require experimental validation in order to compare with plants and other algae. We did not find any evidence of large copy number variations of sugar transporter genes in *Phaeocystis* genomes compared to other haptophytes, which could have been a first indication of a genomic footprint to explain the predominance of this genus in symbiosis. This hypothesis has already been explored and validated in symbiotic microalgae: Symbiodiniaceae clades presented enriched functions related to transmembrane transport in their genomes compared to other non-symbiotic dinoflagellates, especially for the major facilitator superfamily (PF07690) [80]. This genomic characterization of the *Phaeocystis* transportome generates fundamental knowledge on this key marine phytoplankton taxon and is an essential step for unveiling the expression dynamics of sugar transporter genes in symbiosis.

Algal transportome is significantly remodeled in symbiosis

To reveal which sugar transporters might play a role in symbiosis, we assessed their gene expression based on single-holobiont transcriptomic analyses. More specifically, we compared the expression of transporter genes of the microalga *P. cordata*

between free-living (four and five culture replicates in exponential and stationary growth phases, respectively) and symbiotic conditions (17 holobionts representing five host species collected in the Mediterranean Sea, Fig. S1) through a Differential Expression (DE) analysis (Fig. 2). Each sample was frozen at the same period of the day (late evening, 7 p.m.). About 75 million of reads were obtained per holobiont sample, producing a total of 1950 billion of reads in this study. A de novo reference transcriptome from total RNA sequences of cultured *P. cordata* was built and used to quantify gene expression.

Before comparing the expression of the transportome between the free-living and symbiotic stages, we assessed whether the transportome of free-living *Phaeocystis* cells maintained in culture varies with respect to the growth phase (i.e. exponential vs stationary phase). Only 3.3% of the transporters were found to be differentially expressed between exponential and stationary phase, indicating that the expression of the transportome is not drastically modified (Table S2). We therefore considered hereafter both growth phases as free-living replicates (nine in total) to compare with the symbiotic stage.

From the 2806 transporters genes considered as expressed in this analysis (sum of normalized read counts >10 in all replicates), 26% (724 genes) were found to be exclusively expressed in free-living and 10% (267 genes) exclusively expressed in symbiosis (Table S3: “Exp FL Symb”). A principal component analysis (PCA) of the DESeq2 dataset showing the gene expression variance revealed: (i) a clear separation between symbiosis and free-living samples; (ii) a high variance in expression of all genes across symbiotic replicates, and (iii) clustering of expression of transporter genes in symbiotic samples (even if a lower part of the variance—32%—is explained by the first two dimensions of the PCA for transporter genes compared to all genes—60%, Fig. 2A and B). We verified this clustering pattern by using different subsets of expressed genes with similar numbers of genes as controls (Fig. S3). These results show the existence of two distinct transportomes of the microalga *Phaeocystis* expressed in the symbiotic and free-living stages.

Compared to the free-living stage, 42% of the transportome was significantly remodeled in symbiosis with 982 differentially expressed genes (Fig. 2C, Table S3: “UP-DOWN global”). Among those, 33% (768 genes) were downregulated and 9% (214 genes) were upregulated in symbiosis (Table S3: “UP-DOWN global”). These numbers are higher than the ones found in a symbiotic dinoflagellate (*Breviolum*), and with an opposite trend: 213 upregulated and 167 downregulated [25]. We explain this remodeling of *Phaeocystis* transportome in symbiosis by a significant global decrease of the transporter gene expression (normalized read counts, Wilcoxon rank sum test, P -value < .01, Fig. 2C) and high positive fold changes for some transporter genes (Fig. 2D, aquaporin PF00230 with $\log_2FC = 26.11$, Table S3: “Res table DE”). Note that 58% of the algal transportome remained expressed in symbiosis but without differential expression. Therefore, these results suggest that many algal transporters could be less required in symbiosis likely due to the transition from the ocean to the host microhabitat, but some transporters could be specifically induced in symbiosis with high transcriptional activity in response to metabolic changes within a host and potentially enable the metabolic connectivity between the two partners.

Expression of the algal sugar transporters in symbiosis

We focused on the expression of sugar transporter genes of the microalga in symbiosis. From our dataset, 261 genes representing

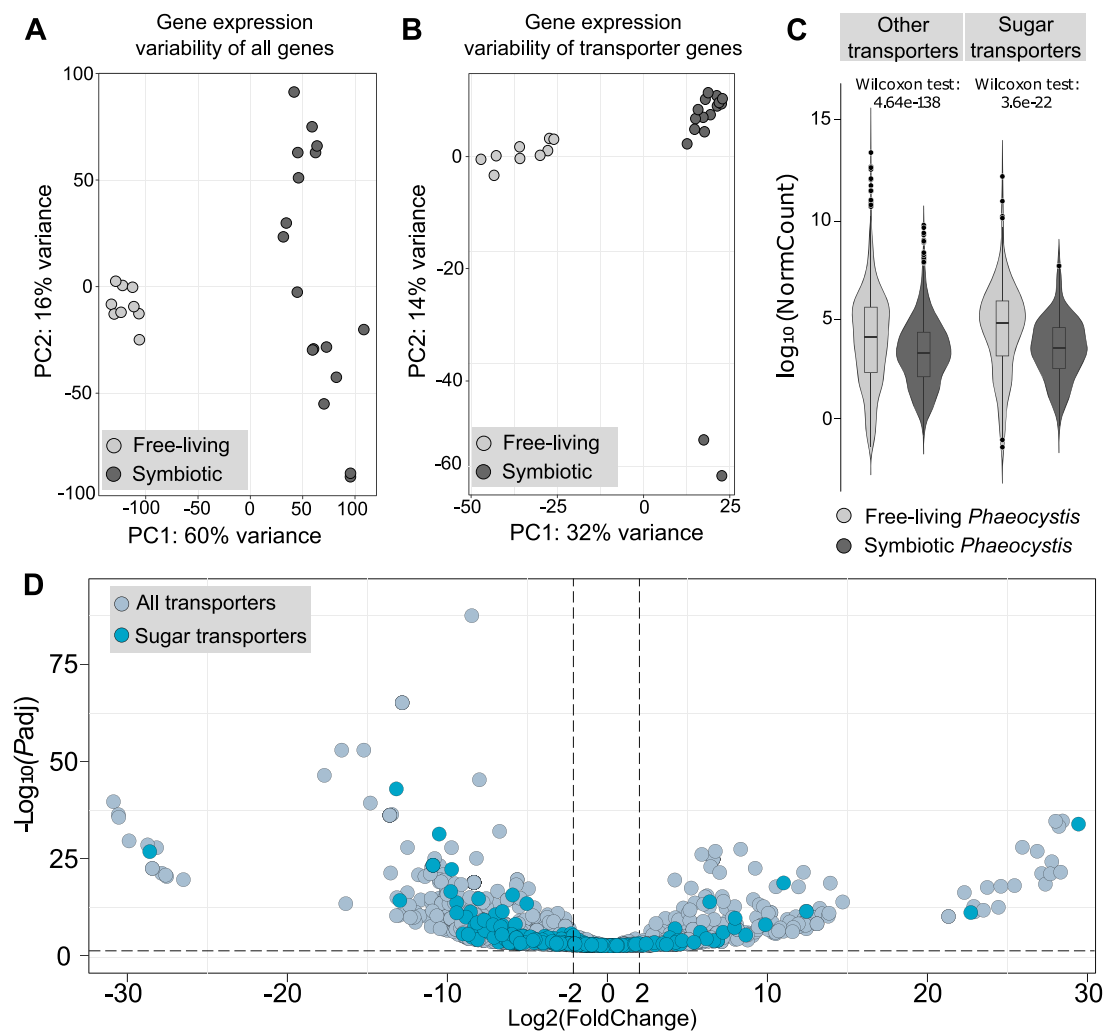


Figure 2. Expression of algal transporter genes between the free-living and symbiotic stages of the microalga *P. cordata*. (A) PCA of gene expression variance between free-living and symbiotic *P. cordata*, including all expressed genes; X-axis represent variance across conditions and y-axis across replicates within each condition. (B) PCA of expression variance of the 2806 transporter genes when comparing free-living and symbiotic *P. cordata*. (C) Comparison of normalized read counts of the sugar (right) and all other transporter (left) genes between free-living and symbiotic *P. cordata*. (D) Volcano plot showing Log₂ (fold change) of up- and downregulated transporter genes of symbiotic *Phaeocystis* compared to the free-living stage, including sugar transporters and other transporters (gray circles; DESeq2 analysis, log₂FC ≥ 2, Padj < .05; see Table S3).

eight Pfams were found to be expressed (out of the 330 sugar transporter genes in the reference transcriptome; Table 1 and Table S3 “UP-DOWN global” and “*P. cordata* SugarTR Anno”). At the Pfam level, we observed that five sugar transporter families presented a global downregulation of gene expression (Figs 3A and S4). Yet, at the gene level, some transporters presented a high upregulation within each Pfam. Among the 36% of sugar transporters remodeled in symbiosis, 8% (19 genes) were found as upregulated and 28% (74 genes) downregulated (Table 1, Figs 2D, 3A, and S4). Note that 64% (167 genes out of the 259) of the sugar transporter genes were still expressed in symbiosis (named “neutral” in Table 1). Among the 19 up-regulated genes in symbiosis, we found nine TPTs (Triose Phosphate Transporters, PF03151, average log₂FC=7.5), two aquaporins (PF00230, average log₂FC=18.5), two monosaccharide transporters (PF00083, average log₂FC=4.8), two MFS/sugar transport protein (PF13347, average log₂FC=5.4), three Nucleotide sugar transporters (NSTs; PF04142, average log₂FC=6.5), and one gene from PF07690 (annotated as Glycerol-3-P transporter, average log₂FC=5.4; Fig. 3B, Table 1). Note that these Pfams are the same that were found upregulated in the study of

Maor-Landaw et al. 2020 [25], translating Uniprot IDs in Pfam accession numbers. These transporters therefore contribute to the significant remodeling and specialization of the algal sugar transcriptome in symbiosis, and potentially play a key role in the flux and exchange of sugars.

Concerning the TPTs, only nine out of 96 genes (9.4%) were upregulated and 66% were still expressed in symbiosis. It is possible that the observed upregulation of some TPTs can be linked to the multiplication of plastids in symbiosis (from two when free-living to up to 60 plastids when symbiosis [34]) and would ensure enhanced sugar export into the cytosol. The most upregulated transporter genes correspond to two aquaporins (PF00230, log₂FC of 26.1.1 and 10.9; Fig. 3B, Table 1, Table S3). This type of aquaporin, also known as glycerol facilitator (*GlpF*), was found to be involved in two benthic photosymbioses and suggested to be involved in glycerol transport [26, 27]. The three upregulated transporter genes with glycerol as putative substrate (two genes of PF00230 and one gene of PF07690) raise the hypothesis that this metabolite can be important for the carbon metabolism of the holobiont and possibly transported to the host. Two other upregulated genes corresponded to putative

Table 1. Number of *P. cordata* sugar transporter genes identified as differentially expressed in symbiosis within each Pfam family.

	Pfam	Pfam description	Down	Neutral	UP	Total
Sugar transporters	PF00083	Sugar (and other) transporter	13	28	2	43
	PF03083	Sugar efflux transporter for intercellular exchange	1	5	0	6
	PF03151	Triose-phosphate transporter family	19	56	10	85
	PF04142	Nucleotide-sugar transporter	10	30	2	39
	PF07690	Major facilitator superfamily	2	9	2	13
	PF00230	Major intrinsic protein	1	6	2	13
	PF13347	MFS/sugar transport protein	2	5	1	7
	PF00474	Sodium/glucose cotransporter	0	1	0	1
	PF00892	GDP-fucose transporter	0	1	0	1
	PF06800	Sugar transport protein	0	1	0	1
	PF08489	UDPxylose/SugarPhosphate translocator	2	0	0	2
	-	L-arabinose	1	0	0	1
	-	GDP-fucose	0	6	0	7
-	GDP-mannose	0	4	1	4	
Total			51	152	19	223

Note that “neutral” indicates sugar transporter gene expressed in symbiosis, but not significantly up- or downregulated compared to the free-living stage with $\log_2FC \geq 2$, $Padj < .05$ criteria.

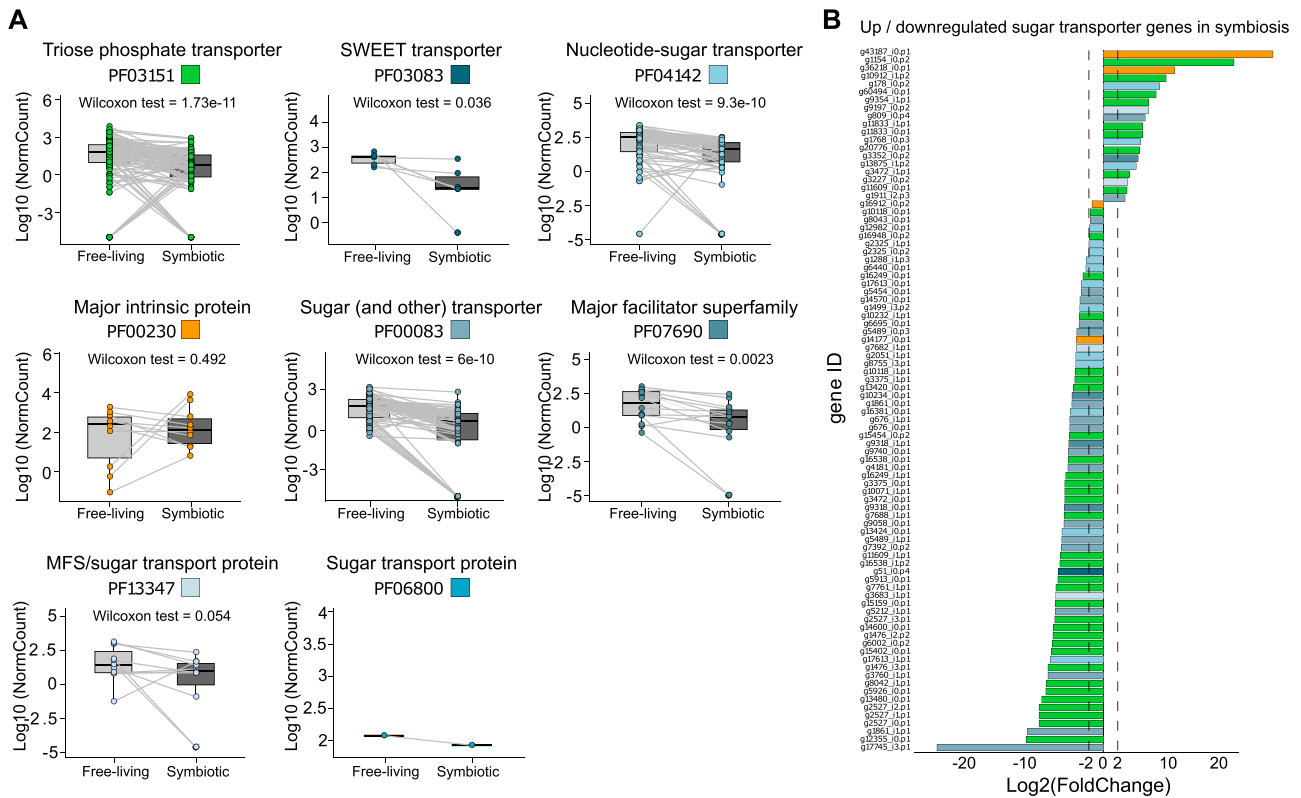


Figure 3. Expression of sugar transporter genes between the free-living and symbiotic *P. cordata* at the gene and Pfam level. (A) Pairwise comparison of the normalized read counts of sugar transporter genes of the eight Pfam families (shown by different colors) between free-living and symbiotic *P. cordata* (Wilcoxon rank sum test, sum of read counts >10 over all replicates). Each circle and line represents one sugar transporter gene. (B) Distribution of \log_2 fold change for up- and downregulated sugar transporter genes in symbiotic *Phaeocystis* when compared to free-living ($\log_2FC > 2$, $Padj < .05$).

transporters of monosaccharides (PF00083), with assignment to GLUT proteins (Fig. S5 and Table S1: “GLUT Characterization”). One of these two GLUT proteins was predicted to be localized at the cell membrane (Table S3, “SubcellLoc SugarTR_UP”). Four SWEET transporter genes (PF03083) were also expressed in symbiosis (\log_2FC ranging between -6.9 to 0.68), but not upregulated. The two upregulated MFS/sugar transport proteins (PF13347, $\log_2FC=5.4$) could also play a role in sugar flux as shown in plants [77]. This transcriptomic analysis from freshly collected holobionts allowed us to reveal the sugar

transportome expressed in the symbiotic microalga and identify candidate genes for future functional characterizations. To have an alternative line of evidence, we investigated the expression of this algal transportome in situ, exploiting metatranscriptomic data collected in the Mediterranean Sea.

In situ sugar transportome expression of the microalga *Phaeocystis* in the Mediterranean Sea

Using the Tara metatranscriptomic dataset from the Mediterranean Sea, we evaluated the expression of sugar transporter

genes of the microalga *Phaeocystis* in two size fractions (small: 0.8–5 μm ; and large: 180–2000 μm) collected in surface waters of six stations from the Tara Oceans expedition ([59], Fig. 4A). *Phaeocystis* reads were specifically recruited in the metatranscriptome dataset based on stringent criteria (sequence homology and coverage thresholds, see Methods and supplemental Figs S6 and S7). The small size fraction mainly corresponds to the free-living stage of *P. cordata* (4 μm in size [81]) whereas its symbiotic stage within acantharians is mainly detected in the large size fraction (note that the Mediterranean species, *P. cordata*, does not form colonies [82]). From this metatranscriptomic dataset, we identified 270 sugar transporters with a difference between the large (123 genes) and small (266 genes) size fraction (Fig. 4B). This can be partially explained by the lower abundance of *Phaeocystis* transcripts in the 180–2000 μm fraction that might have been diluted and so less sequenced due to the high abundance of transcripts from large multicellular organisms (zooplankton).

In order to normalize and compare gene expression between the two size fractions, we calculated the ratio between the expression (TPM) of the 270 sugar transporter genes and a selected set of 149 housekeeping genes (e.g. ribosomal proteins, tubulin, ATP synthase...) whose expression levels were expected to correspond to basic cellular activity (see Materials and methods and Table S4: “sugarTR counts”). Based on this normalization method, we found 24 sugar transporter genes with a higher mean expression value in the large size fraction compared to the small one: one SWEET gene, twelve TPTs, six NSTs, three aquaporins, one GLUT, and one member for the MFS/sugar transporter protein PF13347 (Fig. 4B, Table S4: “Large_supp_small”). Eighteen out of the nineteen sugar transporter genes found as upregulated in symbiosis (Fig. 3B, single-holobiont transcriptomic analysis) were also detected in both size fractions of the metatranscriptomic dataset. Of these, six of them were found to present a higher TPM value in the large size fraction and correspond to two aquaporin PF00230 genes, the transporter from PF07690, two TPTs, and one PF04142 (Fig. 4C, Table S4). Note that the two aquaporin genes identified here correspond to the genes that presented the highest positive fold change values in symbiosis in the differential expression analysis from isolated holobionts (Fig. 3B). This in situ metatranscriptomic analysis provides an ecological context for our experimental study, and further confirms some sugar transporter candidates as key players in symbiosis, such as TPTs and aquaporin.

Dynamic expression of the algal sugar transportome in symbiosis during the day

It is well established that photosynthesis and central carbon metabolism depend on the circadian rhythm and light conditions [83–85]. Therefore, in order to further understand the metabolic connectivity, we investigated the transcriptional dynamics of the sugar transportome of symbiotic *Phaeocystis* by harvesting acantharia hosts at three different times of day and light exposure periods: (i) morning (9 a.m., after 1 h light exposure), (ii) evening (7 p.m., after 10 h light exposure), and (iii) dark-evening (7 p.m., after an incubation in darkness for 24 hours). The dark-evening condition corresponds to a situation where holobionts, and thus microalgae experience a non-photosynthetic day (absence of light). In total, we found 209 sugar transporter genes expressed in these three conditions, representing 96% (214/223) of the sugar transportome (Table S5, Fig. S8, Table 1). Overall, 28% (60 genes) of sugar transporters were found to be expressed in the morning, 43% (91 genes) expressed in the evening and 29% (63 genes) in the dark-evening (Table S5). Among them, some were exclusively

expressed in the morning (18), evening (43) or dark-evening (16; Fig. 5A, Table S5). These results demonstrate that many sugar transporter genes of the symbiotic microalga tend to be induced during the day. From the comparison of holobionts collected in the evening and submitted or not to darkness (dark-evening), we found 53% (113/214) of genes downregulated when incubated in the dark ($FC < -2$, Table S5). 34% (72/214) were still expressed in the holobionts exposed to darkness and thus, their expression does not seem to be linked to the presence of light. These results show that the majority of sugar transporter expression of the symbiotic microalga is modulated by light conditions.

At the Pfam level, we found specific expression patterns modulated by either light or period of the day (Fig. 5B, Table S5). For instance, the expression of TPTs and Glycerol 3-Phosphate transporter (PF07690) tended to be modulated only by light since they were significantly more expressed in evening vs dark-evening conditions and did not show significantly higher expression between morning and evening (Wilcoxon rank sum test, P -value $< .05$, Fig. 5B, Table S5). On the contrary, transcription of sugar hexose transporters (PF00083) seemed to be more regulated by the period of the day as shown by a significant higher expression in the evening compared to morning but not differentially expressed between evening and dark-evening conditions (Wilcoxon P -value $< .05$, Fig. 5B, Table S5). NSTs seemed to be regulated by both parameters (light and period of the day) as they were found to be significantly more expressed in the evening vs morning, and dark-evening vs evening (Wilcoxon P -value $< .01$, Fig. 5B, Table S5). MFS/sugar transport protein (PF13347) genes tended to present a higher expression in the dark (Fig. 5B, Table S5). SWEET genes were not differentially expressed between the three conditions, yet two pairs of genes seemed to present opposite patterns (more expressed in the morning or in the dark). Generally, aquaporin genes (PF00230) exhibited a lower expression in the darkness and two of them were only expressed in the evening, after the normal daylight exposure. These results show specific transcriptional patterns of sugar transporters in response to light (PF07690, PF03151, PF13347), to the period of the day (PF00083) or both parameters (PF04142, PF03083).

We also paid attention to the dynamics of the sugar transporter genes found to be upregulated in symbiosis from our holobiont transcriptomes. The nine upregulated TPTs in symbiosis exhibited several transcriptional patterns: two genes exclusively expressed in the morning and two genes exclusively in the evening; in addition, two genes had a higher expression in the evening compared to morning, and six genes had a higher expression in light (evening) compared to dark-evening (Fig. 5C, Table S5). This suggests that different TPT genes might have specific roles at different periods of the day and this could depend on their subcellular localization. GLUT and aquaporin genes upregulated in symbiosis showed a higher expression in morning vs evening, or dark-evening vs evening, raising two hypotheses: (i) the transcription is activated in the morning to produce transporters during the day or (ii) transcription mainly takes place in the dark for sugar excretion at night. Further studies should increase the temporal resolution during a day-night cycle to fully reveal the dynamics of the transportome expression of the symbiotic microalga.

Discussion

This study improves our understanding of the molecular players that are potentially involved in the carbon metabolism, and metabolic connectivity between the symbiotic microalga *Phaeocystis* and its acantharian host. We found that *Phaeocystis* species

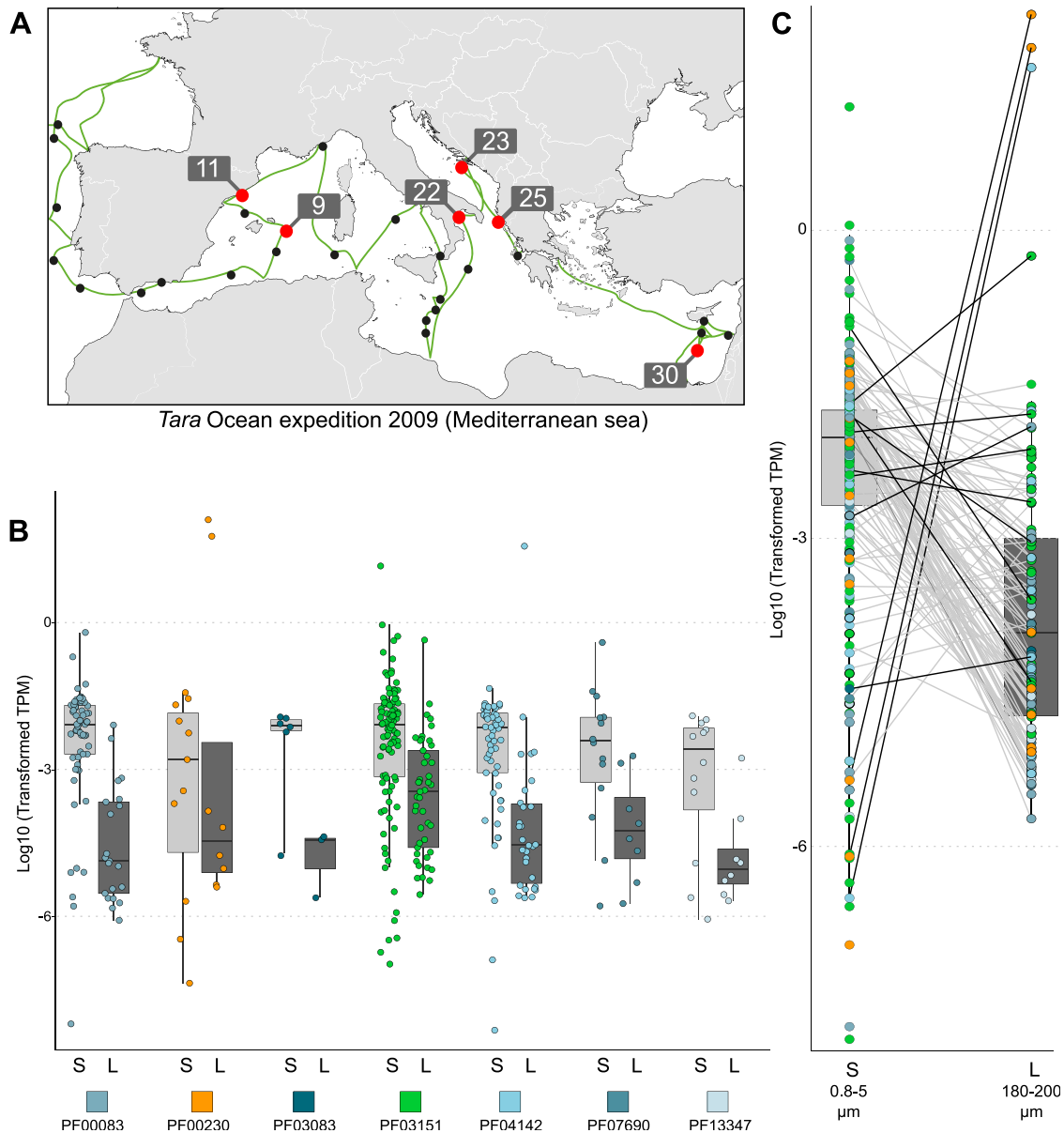


Figure 4. *In situ* expression of sugar transporter genes of the microalga *P. cordata* in the Mediterranean Sea based on environmental metatranscriptomic data. (A) Geographic map showing the six different sampling stations of the *Tara* oceans expedition analyzed in this study. (B) Comparison of the TPM (transcript per million) values for sugar transporter genes between the small (0.8–5 μm , S) and large (180–2000 μm , L) size fractions for each Pfam (each point corresponds to the TPM value of one sugar transporter gene). (C) Comparison of TPM values of sugar transporter genes between the small and large size fractions including those identified as upregulated in the single-holobiont transcriptomes (see Fig. 3). In B and C, the TPM value of each sugar transporter gene was normalized by the expression of housekeeping genes (see Materials and methods).

share a conserved sugar transportome among haptophytes at the Pfam level with few differences in gene copy number. Therefore, this genomic analysis did not reveal a specific sugar transportome linked to the symbiotic life stage of the microalga *Phaeocystis*, compared to non-symbiotic haptophytes. This can be explained by the fact that *Phaeocystis* symbionts are not vertically transmitted across host generations, do not depend on symbiosis for survival, and genome evolution would rather occur in the extensive free-living population [5]. Our study shows that the capacity of the microalga *Phaeocystis* to be in symbiosis may be rather due to the large plasticity of the transportome expression with 42% of transporter genes of metabolites and nutrients being differentially expressed. This suggests a drastic change in the flux and homeostasis of metabolites and nutrients in the symbiotic

microalgae. More specifically, downregulation of most transporter genes along with high expression of a few ones suggests (i) lower trafficking of metabolites linked to the intracellular life stage (perhaps due to the arrested cell division), and (ii) specialization toward some metabolite fluxes putatively beneficial for the host. The transcriptional plasticity of the algal sugar transportome not only takes place during the free-living-to-symbiosis transition but also throughout the day. This reveals the complex dynamics of the carbon homeostasis and fluxes in the holobiont system.

Among the 19 sugar transporters of the microalga *Phaeocystis* upregulated in symbiosis, we found two GLUT and two aquaporin genes, which were also found to be more expressed in the large size fraction of environmental metatranscriptomes. This study provides further evidence that GLUT and aquaporin transporters,

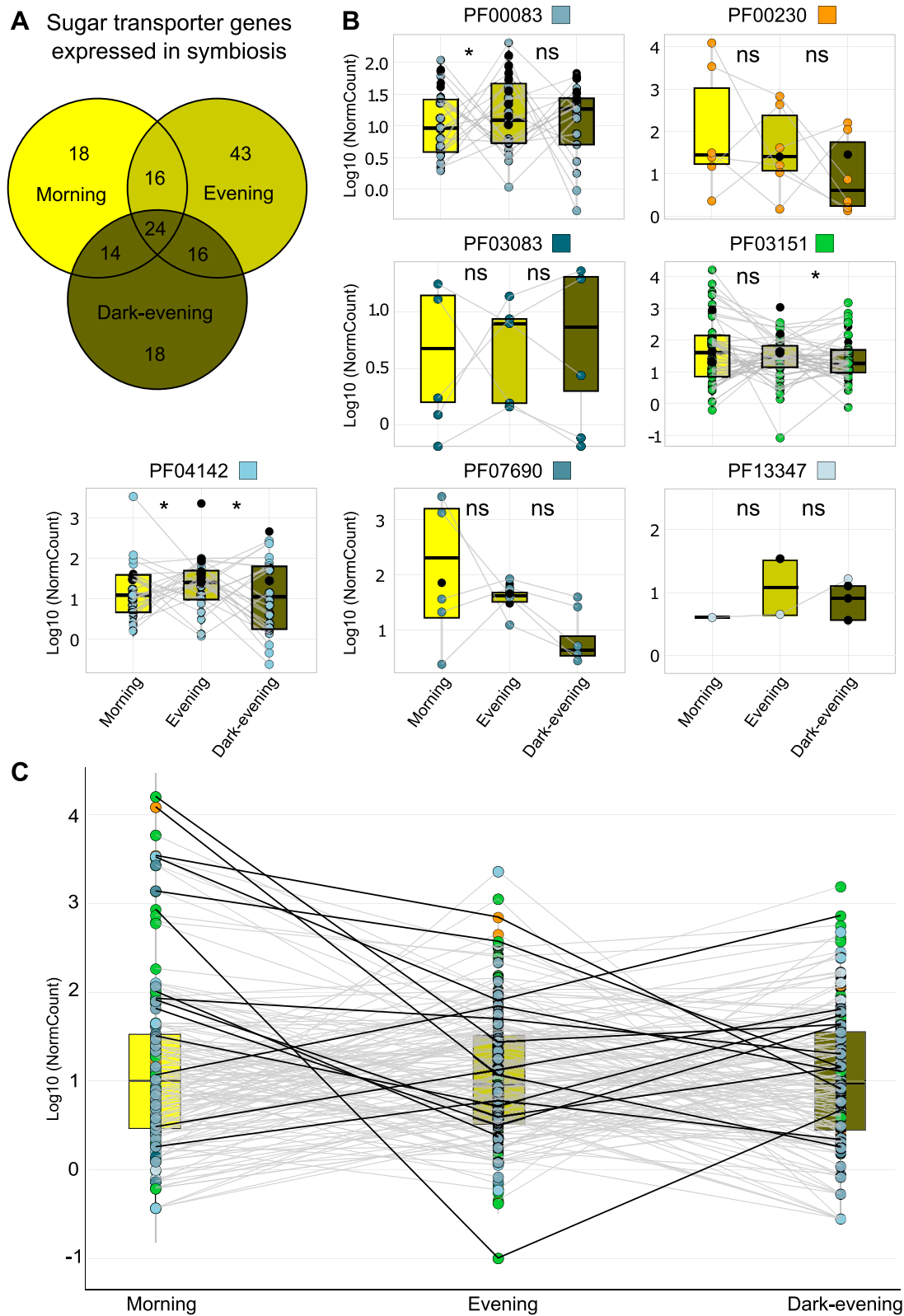


Figure 5. Temporal dynamics of sugar transportome expression in the symbiotic microalga *P. cordata*. (A) Venn diagram showing the number of sugar transporter genes expressed in one or different conditions (morning, evening and dark-evening; DESeq2 normalized read counts >10 for one condition and < 10 for the other two conditions). (B) Comparison of the normalized read counts of sugar transporter genes of the different Pfam families between morning, evening and dark-evening conditions; Wilcoxon rank sum tests are represented as ns (non-significant) and * (significant <0.05) for morning/evening and evening/dark-evening comparisons. The black circles correspond to the genes specifically expressed in one condition (in Venn diagram). (C) Dynamic of the sugar transporter genes found upregulated in symbiosis (Fig. 3B) across the three conditions (morning, evening and dark-evening, comparison of mean values of normalized read counts).

which are also upregulated in other photosymbiotic hosts [26, 27], play a key role in symbiosis. Similarly, the higher expression of a SWEET gene in this large size fraction suggests that this transporter may also be involved in metabolic connectivity in this planktonic symbiosis, as shown for anemone/dinoflagellate symbiosis [28].

The diversity of transporters and their expression patterns raise the hypothesis that several algal carbohydrates (glucose, glycerol) might be transferred to the host at different temporal windows. Future functional characterization (e.g. expression in heterologous systems) of the candidate sugar transporters revealed here will be essential to fully understand the role of these transporters in symbiosis. Overall, this study expands the list of holobionts using similar transporter genes and raises the hypothesis of a convergence for carbon exchange mechanisms in photosymbiosis.

Acknowledgements

We are deeply grateful toward Adria Auladell and David J Richter for their collaboration and help on metatranscriptomic analysis. We thank also Zoltan Füssy and Andrew E Allen for providing us the predicted proteome from *Phaeocystis cordata* genome they assembled and annotated. We thank Annelien Verfaillie and Alvaro Cortes from the Genomics Core platform in Leuven. We are grateful to the Roscoff Bioinformatics platform ABiMS (<http://abims.sb-roscoff.fr>), part of the Institut Français de Bioinformatique (ANR-11-INBS-0013) and BioGenouest network, for providing help for computing HECTAR subcellular localization prediction. We thank Margaret Mars Brisbin for help with bioinformatic pipeline construction and Noan LeBescot for assisting with figure preparation.

Author contributions

CJ and JD conceived, planned the research, and wrote the manuscript; CJ, JD, and FC performed sampling and experiments sampling; CJ performed data analysis, figures generation, and drafted the first manuscript; AA, EP, and DR performed data analysis from metatranscriptomics of *Tara* data. All authors participated in discussions interpreting results, provided comments, and approved the final version.

Supplementary material

Supplementary material is available at *The ISME Journal* online.

Conflicts of interest

The authors declare no competing interests.

Funding

Research was supported by CNRS and ATIP-Avenir program funding, and by the European Union (BIOcean5D—GA#101059915 and ERC—SymbiOCEAN—101088661). This project has received funding from the European Union's Horizon 2020 research and innovation program under grant agreement no. 824110 for the sequencing (EASI Genomics). This project has received funding from the European Union's Horizon 2020 research and innovation program under grant agreement no. 824110 for the sequencing (EASI Genomics). Z.F. and A.A. were funded by National Oceanic and Atmospheric Administration grant NA19NOS4780181 (to

A.E.A.), the National Science Foundation (NSF-OCE-1756884 to A.E.A.), and the Simons Collaboration on Principles of Microbial Ecosystems (PriME; grant ID: 970820 to A.E.A.). Their work (proposal: 10.46936/10.25585/60001426) conducted in the US Department of Energy Joint Genome Institute (<https://ror.org/04xm1d337>), a DOE Office of Science User Facility, is supported by the Office of Science of the US Department of Energy operated under contract no. DE-AC02-05CH11231. A.A. and D.J.R. received funding from the European Research Council (ERC) under the European Union's Horizon 2020 research and innovation program (grant agreement 949745—GROWCEAN—ERC-2020-STG) and from the Departament de Recerca i Universitats de la Generalitat de Catalunya (exp. 2021 SGR 00751).

Data availability

All raw sequencing data generated for this manuscript are available from the NCBI SRA under accession PRJNA1159218.

References

1. Archibald JM. Genomic perspectives on the birth and spread of plastids. *Proc Natl Acad Sci* 2015;**112**:10147–53. <https://doi.org/10.1073/pnas.1421374112>
2. Keeling PJ. The endosymbiotic origin, diversification and fate of plastids. *Philos Trans R Soc B Biol Sci* 2010;**365**:729–48. <https://doi.org/10.1098/rstb.2009.0103>
3. Burki F, Sandin MM, Jamy M. Diversity and ecology of protists revealed by metabarcoding. *Curr Biol* 2021;**31**:R1267–80. <https://doi.org/10.1016/j.cub.2021.07.066>
4. Decelle J, Stryhanyuk H, Gallet B et al. Algal Remodeling in a ubiquitous planktonic Photosymbiosis. *Curr Biol CB* 2019;**29**:968–978.e4. <https://doi.org/10.1016/j.cub.2019.01.073>
5. Decelle J. New perspectives on the functioning and evolution of photosymbiosis in plankton. *Commun Integr Biol* 2013;**6**:e24560. <https://doi.org/10.4161/cib.24560>
6. De Vargas C, Audic S, Henry N et al. Eukaryotic plankton diversity in the sunlit ocean. *Science* 2015;**348**:1261605. <https://doi.org/10.1126/science.1261605>
7. Bronstein JL. The exploitation of mutualisms. *Ecol Lett* 2001;**4**:277–87. <https://doi.org/10.1046/j.1461-0248.2001.00218.x>
8. Davy SK, Allemand D, Weis VM. Cell biology of cnidarian–dinoflagellate symbiosis. *Microbiol Mol Biol Rev* 2012;**76**:229–61. <https://doi.org/10.1128/MMBR.05014-11>
9. LeKieffre C, Jauffrais T, Geslin E et al. Inorganic carbon and nitrogen assimilation in cellular compartments of a benthic kleptoplastic foraminifera. *Sci Rep* 2018;**8**:10140. <https://doi.org/10.1038/s41598-018-28455-1>
10. Kopp C, Wisztorski M, Revel J et al. MALDI-MS and NanoSIMS imaging techniques to study cnidarian–dinoflagellate symbioses. *Zoology* 2015;**118**:125–31. <https://doi.org/10.1016/j.zool.2014.06.006>
11. Decelle J, Veronesi G, LeKieffre C et al. Subcellular architecture and metabolic connection in the planktonic photosymbiosis between Collodaria (radiolarians) and their microalgae. *Environ Microbiol* 2021;**23**:6569–86. <https://doi.org/10.1111/1462-2920.15766>
12. Catacora-Grundy A, Chevalier F, Yee D et al. Sweet and fatty symbionts: photosynthetic productivity and carbon storage boosted in microalgae within a host Preprint at. <https://doi.org/10.1101/2023.12.22.572971>
13. Hambleton EA. How corals get their nutrients. *elife* 2023;**12**:e90916. <https://doi.org/10.7554/eLife.90916>

14. Papina M, Meziane T, van Woesik R. Symbiotic zooxanthellae provide the host-coral *Montipora digitata* with polyunsaturated fatty acids. *Comp Biochem Physiol B Biochem Mol Biol* 2003;**135**: 533–7. [https://doi.org/10.1016/S1096-4959\(03\)00118-0](https://doi.org/10.1016/S1096-4959(03)00118-0)
15. Markell DA, Trench RK. Macromolecules exuded by symbiotic dinoflagellates in culture: amino acid and sugar composition. *J Phycol* 1993;**29**:64–8. <https://doi.org/10.1111/j.1529-8817.1993.tb00280.x>
16. Burriesci MS, Raab TK, Pringle JR. Evidence that glucose is the major transferred metabolite in dinoflagellate–cnidarian symbiosis. *J Exp Biol* 2012;**215**:3467–77. <https://doi.org/10.1242/jeb.070946>
17. Ishii Y, Ishii H, Kuroha T et al. Environmental pH signals the release of monosaccharides from cell wall in coral symbiotic alga. *elife* 2023;**12**:e80628. <https://doi.org/10.7554/eLife.80628>
18. Gordon BR, Leggat W. Symbiodinium–invertebrate symbioses and the role of metabolomics. *Mar Drugs* 2010;**8**:2546–68. <https://doi.org/10.3390/md8102546>
19. Muscatine L. Glycerol excretion by symbiotic algae from corals and *Tridacna* and its control by the host. *Science* 1967;**156**:516–9. <https://doi.org/10.1126/science.156.3774.516>
20. Hillyer KE, Dias DA, Lutz A et al. Metabolite profiling of symbiont and host during thermal stress and bleaching in the coral *Acropora aspera*. *Coral Reefs* 2017;**36**:105–18. <https://doi.org/10.1007/s00338-016-1508-y>
21. Suescún-Bolívar LP, Traverse GMI, Thomé PE. Glycerol outflow in Symbiodinium under osmotic and nitrogen stress. *Mar Biol* 2016;**163**:128. <https://doi.org/10.1007/s00227-016-2899-6>
22. Ruffinatti FA, Scarpellina G, Chinigo G et al. The emerging concept of transportome: state of the art. *Physiology* 2023;**38**: 285–302. <https://doi.org/10.1152/physiol.00010.2023>
23. Banasiak J, Jamruszka T, Murray JD et al. A roadmap of plant membrane transporters in arbuscular mycorrhizal and legume–rhizobium symbioses. *Plant Physiol* 2021;**187**:2071–91. <https://doi.org/10.1093/plphys/kiab280>
24. Sproles AE, Kirk NL, Kitchen SA et al. Phylogenetic characterization of transporter proteins in the cnidarian–dinoflagellate symbiosis. *Mol Phylogenet Evol* 2018;**120**:307–20. <https://doi.org/10.1016/j.ympev.2017.12.007>
25. Maor-Landaw K, van Oppen MJH, McFadden GI. Symbiotic lifestyle triggers drastic changes in the gene expression of the algal endosymbiont *Breviolum minutum* (Symbiodiniaceae). *Ecol Evol* 2020;**10**:451–66. <https://doi.org/10.1002/ece3.5910>
26. Mashini AG, Oakley CA, Grossman AR et al. Immunolocalization of metabolite transporter proteins in a model cnidarian–dinoflagellate symbiosis. *Appl Environ Microbiol* 2022;**88**:e00412–22. <https://doi.org/10.1128/aem.00412-22>
27. Carabantes N, Grosso-Becerra MV, Thomé PE. Expression of glucose (GLUT) and glycerol (GLP) transporters in symbiotic and bleached *Cassiopea xamachana* (Bigelow, 1892) jellyfish. *Mar Biol* 2024;**171**:54. <https://doi.org/10.1007/s00227-023-04374-2>
28. Maor-Landaw K, Eisenhut M, Tortorelli G et al. A candidate transporter allowing symbiotic dinoflagellates to feed their coral hosts. *ISME Commun* 2023;**3**:2730–6151. <https://doi.org/10.1038/s43705-023-00218-8>
29. Decelle J, Colin S, Foster RA. Photosymbiosis in marine planktonic protists. In: Ohtsuka S, Suzaki T, Horiguchi T et al (eds), *Marine Protists: Diversity and Dynamics*. Springer Japan, 2015, pp. 465–500. https://doi.org/10.1007/978-4-431-55130-0_19
30. Decelle J, Probert I, Bittner L et al. An original mode of symbiosis in open ocean plankton. *Proc Natl Acad Sci* 2012;**109**:18000–5. <https://doi.org/10.1073/pnas.1212303109>
31. Mars Brisbin M, Mesrop LY, Grossmann MM et al. Intra-host symbiont diversity and extended symbiont maintenance in photosymbiotic Acantharea (Clade F). *Front Microbiol* 2018;**9**:1998. <https://doi.org/10.3389/fmicb.2018.01998>
32. Poff KE, Leu AO, Eppley JM et al. Microbial dynamics of elevated carbon flux in the open ocean’s abyss. *Proc Natl Acad Sci* 2021;**118**:e2018269118. <https://doi.org/10.1073/pnas.2018269118>
33. Michaels AF. Vertical distribution and abundance of Acantharia and their symbionts. *Mar Biol* 1988;**97**:559–69. <https://doi.org/10.1007/BF00391052>
34. Uwizeye C, Mars Brisbin M, Gallet B et al. Cytoklept in the plankton: a host strategy to optimize the bioenergetic machinery of endosymbiotic algae. *Proc Natl Acad Sci* 2021;**118**:e2025252118. <https://doi.org/10.1073/pnas.2025252118>
35. Grigoriev IV, Hayes RD, Calhoun S et al. PhycoCosm, a comparative algal genomics resource. *Nucleic Acids Res* 2021;**49**:D1004–11. <https://doi.org/10.1093/nar/gkaa898>
36. Allen A, Füssy Z, Lampe R et al. Genome-resolved biogeography of Phaeocystales, cosmopolitan bloom-forming algae Preprint at. <https://doi.org/10.21203/rs.3.rs-4339559/v1>
37. Jones P, Binns D, Chang H-Y et al. InterProScan 5: genome-scale protein function classification. *Bioinformatics* 2014;**30**:1236–40. <https://doi.org/10.1093/bioinformatics/btu031>
38. Saier MH Jr, Reddy VS, Moreno-Hagelsieb G et al. The transporter classification database (TCDB): 2021 update. *Nucleic Acids Res* 2021;**49**:D461–7. <https://doi.org/10.1093/nar/gkaa1004>
39. Mistry J, Chuguransky S, Williams L et al. Pfam: the protein families database in 2021. *Nucleic Acids Res* 2020;**49**:D412–9. <https://doi.org/10.1093/nar/gkaa913>
40. Cantalapiedra CP, Hernández-Plaza A, Letunic I et al. eggNOG-mapper v2: functional annotation, orthology assignments, and domain prediction at the metagenomic scale. *Mol Biol Evol* 2021;**38**:5825–9. <https://doi.org/10.1093/molbev/msab293>
41. Käll L, Krogh A, Sonnhammer ELL. A combined transmembrane topology and signal peptide prediction method. *J Mol Biol* 2004;**338**:1027–36. <https://doi.org/10.1016/j.jmb.2004.03.016>
42. Krogh A, Larsson B, von Heijne G et al. Predicting transmembrane protein topology with a hidden markov model: application to complete genomes. *J Mol Biol* 2001;**305**:567–80. <https://doi.org/10.1006/jmbi.2000.4315>
43. Thumulari V, Almagro Armenteros JJ, Johansen AR et al. DeepLoc 2.0: multi-label subcellular localization prediction using protein language models. *Nucleic Acids Res* 2022;**50**:W228–34. <https://doi.org/10.1093/nar/gkac278>
44. Armenteros JJA, Salvatore M, Emanuelsson O et al. Detecting sequence signals in targeting peptides using deep learning. *Life Sci Alliance* 2019;**2**:e201900429. <https://doi.org/10.26508/lsa.201900429>
45. Gschloessl B, Guermeur Y, Cock JM. HECTAR: a method to predict subcellular targeting in heterokonts. *BMC Bioinformatics* 2008;**9**:393. <https://doi.org/10.1186/1471-2105-9-393>
46. Horton P, Park K-J, Obayashi T et al. WoLF PSORT: protein localization predictor. *Nucleic Acids Res* 2007;**35**:W585–7. <https://doi.org/10.1093/nar/gkm259>
47. Jiang Y, Jiang L, Akhil CS et al. MULocDeep web service for protein localization prediction and visualization at subcellular and suborganellar levels. *Nucleic Acids Res* 2023;**51**:W343–9. <https://doi.org/10.1093/nar/gkad374>
48. Fleet J, Ansari M, Pittman JK. Phylogenetic analysis and structural prediction reveal the potential functional diversity between green algae SWEET transporters. *Front Plant Sci* 2022;**13**:960133. <https://doi.org/10.3389/fpls.2022.960133>

49. Picelli S, Faridani OR, Björklund ÅK et al. Full-length RNA-seq from single cells using smart-seq2. *Nat Protoc* 2014;**9**:171–81. <https://doi.org/10.1038/nprot.2014.006>
50. Vaultot D, Sim CWH, Ong D et al. metaPR: a database of eukaryotic 18S rRNA metabarcodes with an emphasis on protists. *Mol Ecol Resour* 2022;**22**:3188–201. <https://doi.org/10.1111/1755-0998.13674>
51. Bolger AM, Lohse M, Usadel B. Trimmomatic: a flexible trimmer for Illumina sequence data. *Bioinformatics* 2014;**30**:2114–20. <https://doi.org/10.1093/bioinformatics/btu170>
52. Lu J, Salzberg SL. Removing contaminants from databases of draft genomes. *PLoS Comput Biol* 2018;**14**:e1006277. <https://doi.org/10.1371/journal.pcbi.1006277>
53. Bushmanova E, Antipov D, Lapidus A et al. rnaSPAdes: a de novo transcriptome assembler and its application to RNA-Seq data. *GigaScience* 2019;**8**:giz100. <https://doi.org/10.1093/gigascience/giz100>
54. Haas BJ, Papanicolaou A, Yassour M et al. De novo transcript sequence reconstruction from RNA-seq using the trinity platform for reference generation and analysis. *Nat Protoc* 2013;**8**:1494–512. <https://doi.org/10.1038/nprot.2013.084>
55. Simão FA, Waterhouse RM, Ioannidis P et al. BUSCO: assessing genome assembly and annotation completeness with single-copy orthologs. *Bioinformatics* 2015;**31**:3210–2. <https://doi.org/10.1093/bioinformatics/btv351>
56. Langmead B, Salzberg SL. Fast gapped-read alignment with bowtie 2. *Nat Methods* 2012;**9**:357–9. <https://doi.org/10.1038/nmeth.1923>
57. Bray NL, Pimentel H, Melsted P et al. Near-optimal probabilistic RNA-seq quantification. *Nat Biotechnol* 2016;**34**:525–7. <https://doi.org/10.1038/nbt.3519>
58. Love MI, Huber W, Anders S. Moderated estimation of fold change and dispersion for RNA-seq data with DESeq2. *Genome Biol* 2014;**15**:550. <https://doi.org/10.1186/s13059-014-0550-8>
59. Carradec Q, Pelletier E, Da Silva C et al. A global ocean atlas of eukaryotic genes. *Nat Commun* 2018;**9**:373. <https://doi.org/10.1038/s41467-017-02342-1>
60. Quinn TP, Erb I, Gloor G et al. A field guide for the compositional analysis of any-omics data. *GigaScience* 2019;**8**:giz107. <https://doi.org/10.1093/gigascience/giz107>
61. Li Z, Zhang Y, Li W et al. Conservation and architecture of housekeeping genes in the model marine diatom *Thalassiosira pseudonana*. *New Phytol* 2022;**234**:1363–76. <https://doi.org/10.1111/nph.18039>
62. Liu S, Storti M, Finazzi G et al. A metabolic, phylogenomic and environmental atlas of diatom plastid transporters from the model species *Phaeodactylum*. *Front Plant Sci* 2022;**13**:950467. <https://doi.org/10.3389/fpls.2022.950467>
63. Moog D, Nozawa A, Tozawa Y et al. Substrate specificity of plastid phosphate transporters in a non-photosynthetic diatom and its implication in evolution of red alga-derived complex plastids. *Sci Rep* 2020;**10**:1167. <https://doi.org/10.1038/s41598-020-58082-8>
64. Fischer K. The import and export business in plastids: transport processes across the inner envelope membrane. *Plant Physiol* 2011;**155**:1511–9. <https://doi.org/10.1104/pp.110.170241>
65. Moog D, Rensing SA, Archibald JM et al. Localization and evolution of uptative triose phosphate translocators in the diatom *Phaeodactylum tricorutum*. *Genome Biol Evol* 2015;**7**:2955–69. <https://doi.org/10.1093/gbe/evv190>
66. Facchinelli F, Weber AP. The metabolite transporters of the plastid envelope: an update. *Front Plant Sci* 2011;**2**:50. <https://doi.org/10.3389/fpls.2011.00050>
67. Fischer K, Weber A. Transport of carbon in non-green plastids. *Trends Plant Sci* 2002;**7**:345–51. [https://doi.org/10.1016/S1360-1385\(02\)02291-4](https://doi.org/10.1016/S1360-1385(02)02291-4)
68. Misra VA, Wafula EK, Wang Y et al. Genome-wide identification of MST, SUT and SWEET family sugar transporters in root parasitic angiosperms and analysis of their expression during host parasitism. *BMC Plant Biol* 2019;**19**:196. <https://doi.org/10.1186/s12870-019-1786-y>
69. Johnson DA, Hill JP, Thomas MA. The monosaccharide transporter gene family in land plants is ancient and shows differential subfamily expression and expansion across lineages. *BMC Evol Biol* 2006;**6**:64. <https://doi.org/10.1186/1471-2148-6-64>
70. Gerardy-Schahn R, Oelmann S, Bakker H. Nucleotide sugar transporters: biological and functional aspects. *Biochimie* 2001;**83**:775–82. [https://doi.org/10.1016/S0300-9084\(01\)01322-0](https://doi.org/10.1016/S0300-9084(01)01322-0)
71. Orellana A, Moraga C, Araya M et al. Overview of nucleotide sugar transporter gene family functions across multiple species. *J Mol Biol* 2016;**428**:3150–65. <https://doi.org/10.1016/j.jmb.2016.05.021>
72. Chen L-Q, Hou B-H, Lalonde S et al. Sugar transporters for intercellular exchange and nutrition of pathogens. *Nature* 2010;**468**:527–32. <https://doi.org/10.1038/nature09606>
73. An J, Zeng T, Ji C et al. A *Medicago truncatula* SWEET transporter implicated in arbuscule maintenance during arbuscular mycorrhizal symbiosis. *New Phytol* 2019;**224**:396–408. <https://doi.org/10.1111/nph.15975>
74. Manck-Götzenberger J, Requena N. Arbuscular mycorrhiza symbiosis induces a major transcriptional reprogramming of the potato SWEET sugar transporter family. *Front Plant Sci* 2016;**7**:487. <https://doi.org/10.3389/fpls.2016.00487>
75. Roy R, Reinders A, Ward J et al. Understanding transport processes in lichen, Azolla–cyanobacteria, ectomycorrhiza, endomycorrhiza, and rhizobia–legume symbiotic interactions. *F1000Research* 2020;**9**:39. <https://doi.org/10.12688/f1000research.19740.1>
76. Joshi S, Patil S, Hossain MA et al. In-silico identification and characterization of sucrose transporter genes and their differential expression pattern under salinity stress in *Glycine max*. *Plant Stress* 2024;**11**:100314. <https://doi.org/10.1016/j.stress.2023.100314>
77. Liu H-T, Ji Y, Liu Y et al. The sugar transporter system of strawberry: genome-wide identification and expression correlation with fruit soluble sugar-related traits in a *Fragaria × ananassa* germplasm collection. *Hortic Res* 2020;**7**:132. <https://doi.org/10.1038/s41438-020-00359-0>
78. Teng GCY, Boo MV, Lam SH et al. Molecular characterization and light-dependent expression of glycerol facilitator (GlpF) in coccoid Symbiodiniaceae dinoflagellates of the giant clam *Tridacna squamosa*. *Gene Rep* 2022;**27**:101623. <https://doi.org/10.1016/j.genrep.2022.101623>
79. Chin W-C, Orellana MV, Quesada I et al. Secretion in unicellular marine phytoplankton: demonstration of regulated exocytosis in *Phaeocystis globosa*. *Plant Cell Physiol* 2004;**45**:535–42. <https://doi.org/10.1093/pcp/pch062>
80. González-Pech RA, Ragan MA, Chan CX. Signatures of adaptation and symbiosis in genomes and transcriptomes of *Symbiodinium*. *Sci Rep* 2017;**7**:15021. <https://doi.org/10.1038/s41598-017-15029-w>
81. Zingone A, Chrétiennot-Dinet M-J, Lange M et al. Morphological and genetic characterization of *Phaeocystis cordata* and *P. jahonii* (prymnesiophyceae), two new species from the Mediterranean Sea. *J Phycol* 1999;**35**:1322–37. <https://doi.org/10.1046/j.1529-8817.1999.3561322.x>

82. Rousseau V, Chrétiennot-Dinet M-J, Jacobsen A et al. The life cycle of *Phaeocystis*: state of knowledge and presumptive role in ecology. In: Leeuwe MA, Stefels J, Belviso S et al (eds), *Phaeocystis, Major Link in the Biogeochemical Cycling of Climate-Relevant Elements*. Springer Dordrecht, 2007, pp. 29–47.
83. Charrier G, Lacointe A, Améglio T. Dynamic modeling of carbon metabolism during the dormant period accurately predicts the changes in frost hardiness in walnut trees *Juglans regia* L. *Front Plant Sci* 2018;**9**:1746. <https://doi.org/10.3389/fpls.2018.01746>
84. Li Y, Xin G, Wei M et al. Carbohydrate accumulation and sucrose metabolism responses in tomato seedling leaves when subjected to different light qualities. *Sci Hortic* 2017;**225**:490–7. <https://doi.org/10.1016/j.scienta.2017.07.053>
85. Shi Q, Chen C, He T et al. Circadian rhythm promotes the biomass and amylose hyperaccumulation by mixotrophic cultivation of marine microalga *Platymonas helgolandica*. *Biotechnol Biofuels Bioprod* 2022;**15**:75. <https://doi.org/10.1186/s13068-022-02174-2>